

Experimental and Modeling Study of the Oxidation of Xylenes

F. BATTIN-LECLERC, R. BOUNACEUR, N. BELMEKKI, P. A. GLAUDE

Département de Chimie Physique des Réactions, UMR 7630 CNRS, INPL-ENSIC 1, rue Grandville, BP 20451, 54001 Nancy Cedex, France

Received 18 July 2005; revised 17 October 2005; accepted 26 October 2005

DOI 10.1002/kin.20160

Published online in Wiley InterScience (www.interscience.wiley.com).

ABSTRACT: This paper describes an experimental and modeling study of the oxidation of the three isomers of xylene (ortho-, meta-, and para-xylenes). For each compound, ignition delay times of hydrocarbon–oxygen–argon mixtures with fuel equivalence ratios from 0.5 to 2 were measured behind reflected shock waves for temperatures from 1330 to 1800 K and pressures from 6.7 to 9 bar. The results show a similar reactivity for the three isomers. A detailed kinetic mechanism has been proposed, which reproduces our experimental results, as well as some literature data obtained in a plug flow reactor at 1155 K showing a clear difference of reactivity between the three isomers of xylene. The main reaction paths have been determined by sensitivity and flux analyses and have allowed the differences of reactivity to be explained. © 2006 Wiley Periodicals, Inc. *Int J Chem Kinet* 38: 284–302, 2006

INTRODUCTION

Aromatic compounds are present in significant amounts in gasolines (~35%) and diesel fuels (~30%) [1]. Nevertheless, detailed chemical kinetic models for the combustion and the oxidation of aromatic compounds are still scarce and mainly restricted to benzene [2–11] or toluene [12–24]. We have recently published a paper presenting an experimental and modeling study of the oxidation of toluene [24] that we have used as a basis for this work about the oxidation of xylenes.

Xylenes are important components of gasolines (up to 10% for the sum of the three isomers), with high research octane numbers (117.5 for meta-xylene and 116.4 for para-xylene) close to that of toluene

(120) [1]. The existing experimental studies concerning the reactions with oxygen of the three isomers of xylenes have been obtained in a flow reactor [25,26] at ~1150 K, in a rapid compression machine [27,28] between 600 and 900 K and in a single cylinder spark ignition engine [29]. The oxidation of meta- and para-xylenes has also been studied in a jet-stirred reactor [30,31] between 900 and 1300 K and that of para-xylene in a shock tube [30] between 1450 and 1760 K. Qualitative mechanisms explaining the experimental phenomena observed have been proposed [25,28], but, up to now, only one detailed kinetic mechanism has been published in the case of para-xylene [30].

The purpose of this paper is to present new experimental data for the oxidation of ortho-, meta-, and para-xylenes obtained in a shock tube from 1300 to 1820 K and pressures from 6.7 to 9 bar and to propose a mechanism able to model these experimental results, as well as literature data obtained in a flow reactor at ~1150 K [25,26].

Correspondence to: F. Battin-Leclerc; e-mail: frederique.battin-leclerc@ensic.inpl-nancy.fr.

Contract grant sponsor: European Commission.

Contract grant number: EVG1-CT-2002-00072 SAFEKINEX.

© 2006 Wiley Periodicals, Inc.

EXPERIMENTAL IGNITION DELAYS TIMES

As it is already described in detail in previous papers [11,33,34], we will just recall here the main features of this experimental device. The reaction (400 cm long, 7.8 cm i.d.) and the driver (90 cm long, 12.8 cm i.d.) parts of this stainless steel shock tube were separated by two terphane diaphragms, which were ruptured by decreasing suddenly the pressure in the space separating them. The driver gas was helium. The incident and reflected shock velocities were measured by four piezoelectric pressure transducers located along the reaction section.

As in our previous work [11,24,33,34], the temperature and the pressure of the test gas behind the incident and the reflected shock waves were derived from the value of the incident shock velocity by using ideal one-dimensional shock equations.

The onset of ignition was detected by OH radical emission at 306 nm through a quartz window with a photomultiplier fitted with a monochromator at the end of the reaction part. The last pressure transducer was located at the same place along the axis of the tube as the quartz window. The ignition delay time was defined as the time interval between the pressure rise measured by the last pressure transducer due to the arrival of the reflected shock wave and the rise of the optical signal by the photomultiplier up to 10% of its maximum value.

Oxygen (99.5% pure), argon, and helium (both 99.995% pure) were supplied by Alphagaz - L'Air Liquide. Para-xylene (99% pure) was provided by Merck-Schuchardt and ortho-xylene (98% pure) and meta-xylene (97% pure) by Sigma-Aldrich. Fresh reaction mixtures were manometrically prepared every day and mixed using a recirculation pump. Before each introduction of the reaction mixture (from 100 to 400 kPa), the reaction section was flushed with pure argon and evacuated (below 10^{-2} kPa), in order that the residual gas was mainly argon. The study was performed under the following experimental conditions (after the reflected shock):

- ♦ temperature (T) from 1330 to 1800 K;
- ♦ pressure (P) from 6.7 to 9 bar;
- ♦ for each of the three isomers, mixtures (xylene: oxygen: argon in molar percent) were (0.375: 7.875:91.75), (0.375:3.937:95.687), (0.375: 1.969:97.653), and (0.625:6.562:92.812), respectively, which correspond to three different equivalence ratios ($\Phi = 0.5, 1$, and 2) and to two different concentrations of xylene (0.375% and 0.625%) and lead to ignition delay times from 3 to 800 μ s.

Tables I–III and Figs. 1–3 present the experimental results thus obtained.

The scatter of the results is larger than in the cases of benzene [11] or toluene [24]; that is probably due to the lower volatility of xylenes (boiling points between 138 and 142°C) compared to that of toluene (boiling point = 111°C) or benzene (boiling point = 80°C) inducing then more condensation and absorption problems. For the 12 studied mixtures, ignition delay times (τ) decrease when temperature rises and varies exponentially vs. $1000/T$. For each xylene, it is also shown that for a given T , ignition delay times increase with the equivalence ratio of the mixture for a given concentration of hydrocarbon, and slightly decrease with

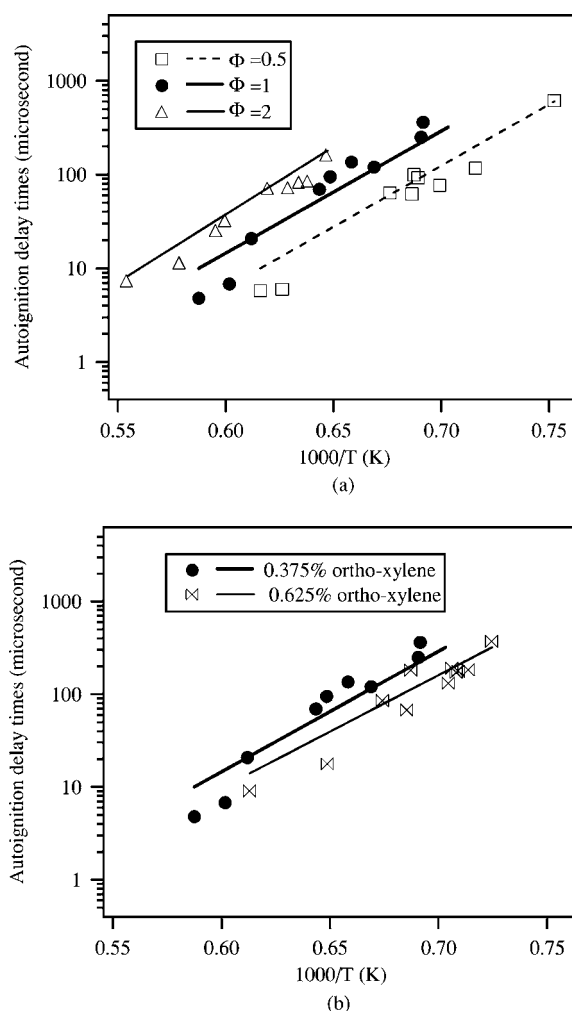


Figure 1 Auto-ignition delay times of ortho-xylene in a shock tube. Semi-log plot of experimental (symbols) and computed (lines) ignition delay times as a function of temperature behind reflected shock wave (a) for different equivalence ratios at 0.375% of xylene and (b) for different hydrocarbon concentrations at $\Phi = 1$.

Table I Mixture Compositions, Shock Conditions, and Ignition Delay Times for ortho-Xylene

Composition (Mole Percent)		P_1 (atm)	P (atm)	V (m/s)	T (K)	τ (μ s)	Composition (Mole Percent)		P_1 (m/s)	P (m/s)	V (atm)	T (K)	τ (s)
C ₈ H ₁₀	O ₂						C ₈ H ₁₀	O ₂					
0.375	3.9375	0.257	7.75	801	1446	361	0.375	1.96875	0.213	7.00	826	1545	159.2
		0.268	8.12	802	1448	249			0.211	7.10	833	1566	84.5
	$\phi = 1$	0.233	7.42	817	1495	120		$\phi = 2$	0.228	7.76	836	1576	82
		0.245	8.00	824	1519	136			0.208	7.14	840	1589	71.3
		0.226	7.58	831	1542	95			0.220	7.72	847	1613	70.5
		0.229	7.76	835	1554	69.5			0.224	8.27	862	1666	32
		0.221	8.11	859	1634	20.7			0.193	7.23	866	1678	25
		0.216	8.13	457	1662	6.8			0.200	7.81	880	1727	11.3
		0.204	7.98	878	1702	4.8			0.184	7.68	901	1803	7.3
0.375	7.875	0.263	7.22	774	1329	617	0.625	6.5625	0.266	8.07	794	1380	367
		0.274	8.17	796	1397	116.7			0.257	7.99	802	1401	181.7
	$\phi = 0.5$	0.2341	7.26	807	1430	76.5		$\phi = 1$	0.243	7.68	805	1410	175.8
		0.245	7.77	814	1451	92.5			0.229	7.23	806	1412	170
		0.230	7.35	815	1455	99.5			0.228	7.22	807	1416	189
		0.220	7.03	817	1457	62			0.232	7.37	808	1419	130.7
		0.223	7.33	823	1479	63.5			0.250	8.29	820	1455	179.3
		0.211	7.8	859	1597	6			0.210	7.02	821	1459	67.5
		0.217	8.26	868	1623	5.8			0.217	7.43	829	1483	84.7
									0.200	7.29	847	1541	17.5
									0.205	8.2	875	1631	9

Note: P_1 is the pressure of the mixture before the shock. V is the speed of the incident wave. P and T are pressure and temperature behind the reflected shock wave. τ is the ignition delay time.

concentration. It is worth noting that in the case of toluene [24], ignition delay times notably increase when the concentration of hydrocarbon increases, while they decrease in the case of benzene [11].

Figure 4 shows that, under the same experimental conditions, the three isomers of xylenes have the similar reactivity.

DESCRIPTION OF THE REACTION MECHANISMS

These three mechanisms, which are available on request, have been written in the CHEMKIN II [32] format and include three parts:

- ◆ A primary mechanism containing 53 reactions for ortho-xylene and para-xylene and 51 reactions for meta-xylene, in which only xylene and oxygen are considered as molecular reactants,
- ◆ A secondary mechanism including 163 reactions for ortho-xylene, 137 reactions for meta-xylene, and 138 reactions for para-xylene, in which the reactants are the main molecular products (apart toluene) formed by the primary mechanism. The primary and secondary mechanisms for ortho-xylene include then 216 reactions.

- ◆ The mechanisms for the oxidation of benzene [11] and toluene [24] are connected to a C₀–C₆ reaction base, which is described in recent papers [33,34].

As shown by Emdee et al. [25,26], benzene and toluene are some important products of the oxidation of xylenes. As previously presented [11], the mechanism for the oxidation of benzene contains 135 reactions and includes the reactions of benzene and of cyclohexadienyl, phenyl, phenylperoxy, phenoxy, hydroxyphenoxy, cyclopentadienyl, cyclopentadienoxy, and hydroxycyclopentadienyl free radicals, as well as the reactions of ortho-benzoquinone, phenol, cyclopentadiene, cyclopentadienone, and vinylketene, which are the primary products yielded. The mechanism for the oxidation of toluene contains 193 reactions and includes the reactions of toluene and of benzyl, tolyl, peroxybenzyl (methylphenyl), alkoxybenzyl, and cresoxy free radicals, as well as the reactions of benzaldehyde, benzyl hydroperoxide, cresol, benzylalcohol, ethylbenzene, styrene, and bibenzyl.

The C₀–C₆ reaction base was constructed from a review of the recent literature and is an extension of our previous C₀–C₂ reaction base [35,33]. This C₀–C₂ reaction base includes the reactions of radicals or molecules including carbon, hydrogen, and oxygen

Table II Mixture Compositions, Shock Conditions, and Ignition Delay Times for meta-Xylene

Composition (Mole Percent)		P_1 (atm)	P (atm)	V (m/s)	T (K)	τ (μ s)	Composition (Mole Percent)		P_1 (m/s)	P (m/s)	V (atm)	T (K)	τ (s)
C ₈ H ₁₀	O ₂						C ₈ H ₁₀	O ₂					
0.375	3.9375	0.246	7.26	795	1426	528	0.375	1.96875	0.250	7.33	794	1440	515
$\phi = 1$		0.274	8.17	799	1437	469	$\phi = 2$		0.258	7.71	804	1470	480
		0.263	7.89	799	1439	299			0.211	0.257	8.04	1501	273
		0.264	8.17	809	1469	288			0.250	8.08	822	1530	322
		0.228	7.06	809	1471	205.8			0.243	7.91	823	1535	249
		0.237	7.78	826	1524	71.5			0.2383	7.77	825	1540	180
		0.250	8.32	829	1537	91.5			0.2173	7.11	826	1543	207
		0.231	7.99	842	1575	61.5			0.237	8.21	843	1600	80.5
		0.238	8.76	860	1636	15.5			0.217	7.43	848	1619	68
		0.235	8.85	867	1663	17.5			0.189	6.65	849	1622	88
		0.212	8.07	870	1675	14			0.243	8.82	856	1647	66.7
$\phi = 0.5$		0.2032	7.76	872	1680	12.5	$\phi = 1$		0.224	8.21	860	1658	48
									0.197	7.6	875	1712	24
		0.270	8.06	797	1399	172.7			0.270	7.74	780	1336	798
		0.249	7.45	798	1402	279			0.230	6.82	787	1359	407
		0.232	7.27	811	1442	136			0.235	7.35	802	1401	308
		0.243	7.66	812	1444	104			0.250	7.82	804	1406	337
		0.257	8.1	813	1446	90.8			0.233	7.45	810	1425	161.7
		0.230	7.34	815	1453	86.7			0.213	7.04	819	1452	157.5
		0.233	7.58	821	1472	58			0.243	8.06	820	1455	167.5
		0.197	6.85	840	1533	15.5			0.263	8.76	821	1459	205.8
$\phi = 0.5$		0.204	7.11	841	1538	22			0.193	6.9	840	1519	70.5
		0.217	7.57	841	1538	22.7			0.210	7.46	842	1524	47.5
		0.224	8.2	856	1586	22.5			0.217	7.82	844	1531	60.5
		0.230	8.55	860	1600	10			0.199	7.22	847	1539	80
		0.197	7.93	885	1681	3.5			0.199	7.87	873	1623	18.0
									0.204	8.1	874	1626	18.5
									0.210	8.40	875	1631	17
									0.204	8.58	892	1685	6.5

Note: P_1 is the pressure of the mixture before the shock. V is the speed of the incident wave. P and T are pressure and temperature behind the reflected shock wave. τ is the ignition delay time.

atoms and containing less than three carbon atoms. The kinetic data used in this base were taken from the literature and are mainly those proposed by Baulch et al. [36] and Tsang et al. [37]. The C₀–C₆ reaction base includes reactions involving C₃H₂, C₃H₃, C₃H₄ (allene and propyne), C₃H₅ (three isomers), C₃H₆, C₄H₂, C₄H₃ (two isomers), C₄H₄, C₄H₅ (five isomers), C₄H₆ (1,3-butadiene, 1,2-butadiene, methylcyclopropene, 1-butyne, and 2-butyne), as well as the formation of benzene [33,34]. Pressure-dependent rate constants follow the formalism proposed by Troe [38], and efficiency coefficients have been included. This reaction base was constructed in order to model experimental results obtained in a jet-stirred reactor for methane and ethane [35], profiles in laminar flames of methane, acetylene, and 1,3-butadiene [33], and shock tube auto-ignition delay times for acetylene, propyne, allene, 1,3-butadiene [33], 1-butyne, and 2-butyne [34].

Heats of formation, specific heats, and entropies of the molecules or radicals considered have been mainly calculated using software THERGAS [39], based on the group and bond additivity methods proposed by Benson [40], and stored as 14 polynomial coefficients, according to the CHEMKIN II formalism [32]. It must be kept in mind that the precision obtained by using group additivity methods to estimate heats of formation is around 2 kcal/mol for molecules and 4 kcal/mol for radicals [40]. Table IV presents, in the case of ortho-xylene the names, the formulae, and the heats of formation of the 35 aromatic species which are not included in the mechanism for the oxidation of benzene [11] and toluene [24]. The heats of formation of the isomers involved in the mechanisms are very close whatever the ortho, meta, or para position of the ring substituents, apart from xylenes. Ortho- and para-xylenes have been considered in their quinoid structure, which is the most stable; the formation of meta-xylene which is

Table III Mixture Compositions, Shock Conditions, and Ignition Delay Times for para-Xylene

Composition (Mole Percent)		P_1	P	V	T	τ	Composition (Mole Percent)		P_1	P	V	T	τ
C ₈ H ₁₀	O ₂	(atm)	(atm)	(m/s)	(K)	(μ s)	C ₈ H ₁₀	O ₂	(m/s)	(m/s)	(atm)	(K)	(s)
0.375	3.9375	0.254	7.93	811	1476	136	0.375	1.96875	0.224	7.03	814	1503	258
		0.210	6.90	825	1522	94			0.200	6.39	818	1518	189
	$\phi = 1$	0.228	7.47	825	1522	100.7		$\phi = 2$	0.203	6.57	823	1533	148
		0.251	8.3	827	1529	93			0.237	7.9	831	1561	135.3
		0.253	8.56	835	1554	80			0.213	7.15	833	1566	137.3
		0.240	8.28	841	1572	64			0.226	7.62	835	1574	123.3
		0.243	8.61	848	1597	38			0.230	7.95	841	1595	77.7
		0.204	7.39	856	1622	21.5			0.218	7.61	845	1608	79.3
		0.245	8.92	857	1628	15			0.221	7.98	855	1641	50
		0.233	8.51	859	1634	18.5			0.195	7.08	857	1652	38.5
		0.201	7.54	865	1657	12.3			0.205	7.8	871	1697	16
		0.197	7.45	867	1663	10			0.197	7.65	877	1718	10
		0.197	7.84	883	1720	8.3							
0.375	7.875	0.251	8.01	815	1453	102	0.625	6.5625	0.257	7.24	776	1324	540
		0.225	7.36	823	1477	102			0.275	8.11	787	1359	343
	$\phi = 0.5$	0.217	7.2	826	1490	89.5		$\phi = 1$	0.239	7.26	794	1381	164.2
		0.238	8.1	835	1517	81.3			0.230	7.42	812	1431	287
		0.201	7.02	841	1538	56			0.220	7.11	813	1435	112
		0.224	7.8	841	1538	48.5			0.239	7.87	818	1450	162.7
		0.217	7.89	853	1578	20.5			0.224	7.8	834	1500	62
		0.237	8.72	857	1592	14.3			0.196	6.97	840	1519	59
		0.210	7.88	863	1608	16			0.225	8.30	851	1554	21
									0.227	8.42	852	1557	23.5
									0.217	8.1	855	1564	27.5
									0.201	7.81	866	1601	11.3

Note: P_1 is the pressure of the mixture before the shock. V is the speed of the incident wave. P and T are pressure and temperature behind the reflected shock wave. τ is the ignition delay time.

in a triplet electronic ground state with a heat of formation, ΔH_f (298 K) = 74 kcal/mol [41], has not been considered.

The primary and secondary mechanisms for the oxidation of xylenes are presented in Table V, as well as the references related to the kinetic data. For shortness in this table, a reaction common to the three isomers is written only once without specifying the type of isomer involved. The mechanism of a given isomer includes all the common reactions, as well as the reactions specific to this type of isomer. The rate parameters for the metatheses are not displayed as they are directly derived from the mechanism for toluene [24] or benzene [11].

Primary Mechanism

The primary mechanism includes the reactions of xylene molecules and of methylbenzyl, methyltolyl, tolyl-methoxyl, and methylcresoxyl free radicals.

Unimolecular decompositions ((1) and (2), numbers referring to Table V) of xylene molecules give either methylbenzyl radicals and H atoms or tolyl and methyl radicals. Reaction (1) is one of the few elementary steps involving xylenes which have been experimentally investigated. Da Costa et al. [42] have shown that the three isomers exhibit a very close reactivity for the decomposition giving H atoms and have proposed the rate expressions that we have used with a A -factor divided by two. For reaction (2), we have considered a rate constant four times higher than that used for the similar reaction in the case of toluene: the presence of two possible methyl groups would account for a factor 2, but a factor 4 leads to a better agreement in simulations related to the shock tube, as reaction (2) is an influential reaction as shown further in the text. The ratio between the A -factors used for reactions (1) and (2) for xylene is then close to that used for toluene. The addition of H-atoms to xylene molecules leads to the formation of toluene and methyl radicals (4), the addition of O-atoms gives H atoms and

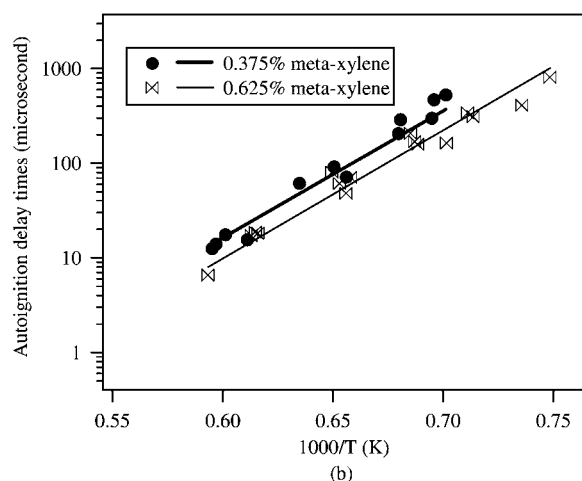
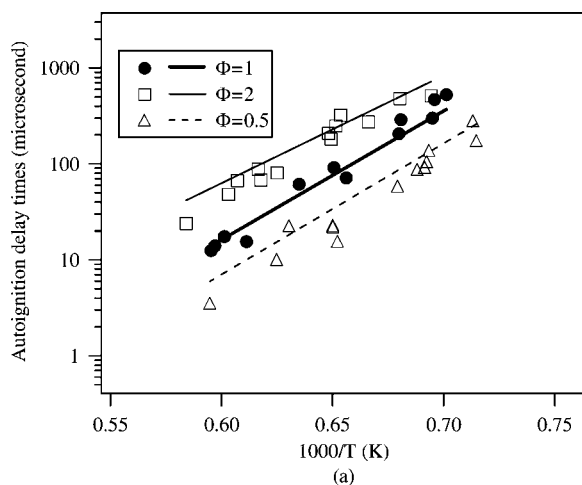


Figure 2 Auto-ignition delay times of meta-xylene in a shock tube. Semi-log plot of experimental (symbols) and computed (lines) ignition delay times as a function of temperature behind reflected shock wave (a) for different equivalence ratios at 0.375% of xylene and (b) for different hydrocarbon concentrations at $\Phi = 1$.

methylcresoxyl radicals (5), and the addition of OH radicals produces H-atoms and methylbenzyl alcohol (6). As in the case of toluene [24], an important part of the reactions of xylene molecules involves the formation of the resonance stabilized methylbenzyl radicals by unimolecular (1) and bimolecular (3) initiations and by metatheses with H-abstraction ((7)–(23)). The rate constants are directly deduced from those of the similar reactions in the case of toluene taking into account the number of abstractable H-atoms; this assumption has been proved correct in the case of the abstraction by H-atoms by a comparison with the experimental value proposed by Hippler et al. [49] ($A = 4 \times 10^{14}$ and $E_a = 8.4$ kcal/mol compared to $A = 4.8 \times 10^{14}$ and $E_a = 8.4$ kcal/mol with our assumption). We have

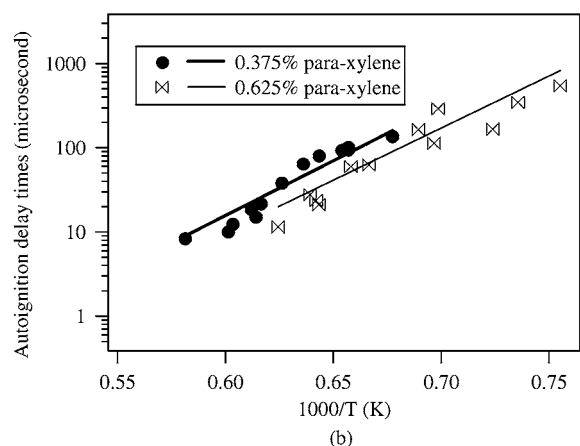
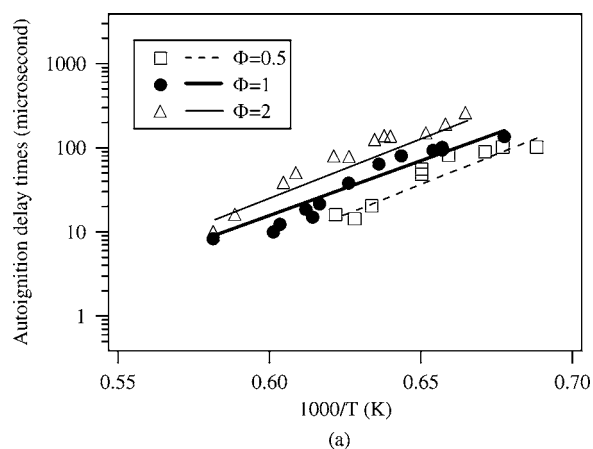


Figure 3 Auto-ignition delay times of para-xylene in a shock tube. Semi-log plot of experimental (symbols) and computed (lines) ignition delay times as a function of temperature behind reflected shock wave (a) for different equivalence ratios at 0.375% of xylene and (b) for different hydrocarbon concentrations at $\Phi = 1$.

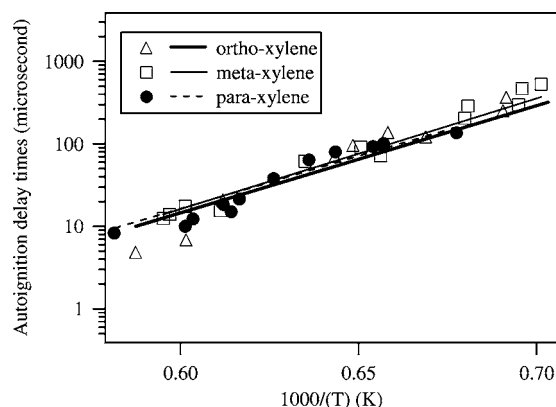


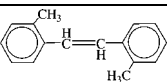
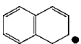
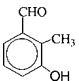
Figure 4 Comparisons between the ignition delay times of the three xylenes. Semi-log plot of experimental (symbols) and computed (lines) delay times as a function of temperature behind reflected shock wave at 0.375% of xylene and $\Phi = 1$.

Table IV Names, Formulae and Heats of Formation for Aromatic Species Involved in Table V

Species	Structure	ΔH_f (298 K)	Species	Structure	ΔH_f (298 K)
<i>o</i> -Xylene (CH ₃ C ₆ H ₄ CH ₃)		4.5	Benzocyclobutene (cCH ₂ CH ₂ C ₆ H ₄)		14.2
<i>m</i> -Xylene (CH ₃ C ₆ H ₄ CH ₃)		4.1	<i>o</i> -Methylbenzyl (CH ₂ C ₆ H ₄ CH ₃)		42.0
<i>p</i> -Xylene (CH ₃ C ₆ H ₄ CH ₃)		4.2	<i>m</i> -Methylbenzyl (CH ₂ C ₆ H ₄ CH ₃)		41.6
Tolualdehyde (CH ₃ C ₆ H ₄ CHO)		-16.2	<i>p</i> -Methylbenzyl (CH ₂ C ₆ H ₄ CH ₃)		41.8
Methylbenzyl hydroperoxide (CH ₃ C ₆ H ₄ CH ₂ OOH)		-15.6	Methyl cresoxyl (OC ₆ H ₃ (CH ₃) ₂)		-1.7
Methylcresol (HOC ₆ H ₃ (CH ₃) ₂)		-37.6	Methyl tolyl (CH ₃ C ₆ H ₃ CH ₃)		65.7
Methylbenzyl alcohol (CH ₃ C ₆ H ₄ CH ₂ OH)		-1.5	Tolyl methoxyl (CH ₃ C ₆ H ₄ CH ₂ O)		19.9
Ethyl toluene (CH ₃ C ₆ H ₄ CH ₂ CH ₃)		-0.1	Methyl benzoyl (CH ₃ C ₆ H ₄ CO)		18.6
Methylstyrene (CH ₃ C ₆ H ₅ CH=CH ₂)		28.4	Methoxy benzyl (CH ₂ C ₆ H ₄ CHO)		21.4
Bimethylbenzyl (C ₁₆ H ₁₈)		34.0	Benzaldehyde methoxyl (CH ₂ OC ₆ H ₄ CHO)		1.1
Mesitylene (C ₆ H ₃ (CH ₃) ₃)		-1.8	Methyl hydroxy benzyl (HOC ₆ H ₃ CH ₃ CH ₂)		-0.1
Dihydronaphthalene (C ₁₀ H ₁₀)		33.2	Tolyl methyl hydroxyl (CH ₃ C ₆ H ₄ CHOH)		1.9
Naphthalene (C ₁₀ H ₈)		36.0	Hydroxy tolyl methoxyl (HOC ₆ H ₃ CH ₃ CH ₂ O)		-22.9
<i>o</i> -Xylylene (CH ₂ C ₆ H ₄ CH ₂)		53.0 ^a	Methyl hydroxy benzoyl (HOC ₆ H ₄ CH ₃ CO)		-24.2
<i>p</i> -Xylylene (CH ₂ C ₆ H ₄ CH ₂)		50.1 ^a	Tolyl ethyl (CH ₃ C ₆ H ₄ CHCH ₃)		33.3
Phthalaldehyde (CHOC ₆ H ₄ CHO)		-35.1	Ditolyl ethyl (C ₁₆ H ₁₇)		67.3

Continued

Table IV Continued

Species	Structure	ΔH_f (298 K)	Species	Structure	ΔH_f (298 K)
Dimethyl stilbene ($\text{CH}_3\text{C}_6\text{H}_4\text{CH}=\text{CHC}_6\text{H}_4\text{CH}_3$)		44.2	Naphthyl (C_{10}H_9)		60.1
Hydroxy tolualdehyde ($\text{CH}_3\text{C}_6\text{H}_4(\text{OH})\text{CHO}$)		-59.0			

Apart from xylenes, xylylenes, and methylbenzyl radicals, only the compounds related to ortho-xylene are presented.

The heats of formation have been calculated by software THERGAS [37] at 298 K in kcal mol^{-1} .

^a Value is taken from Pollack et al. [41].

also considered the formation of methyl tolyl radicals by abstraction of phenylic H-atoms ((24)–(28)), with rate constants deriving from those of the similar reactions in the case of benzene [11].

The reactions common to the three isomers of methylbenzyl radicals are directly derived from those of benzyl radicals: decomposition to form acetylene (29), reaction with oxygen molecules (31), and termination reactions with other radicals ((34)–(39)). By analogy with benzyl radicals, the decomposition (29) would lead to the formation of $\cdot\text{C}_5\text{H}_4\text{CH}_3$ radicals, but Emdee et al. [26] proposed a fast rearrangement of this species to give $\cdot\text{H}$ atoms and benzene. As we consider here only a high-temperature mechanism to model results above 1100 K, we have neglected the formation of methylperoxybenzyl radicals. The reaction of methylbenzyl radicals with oxygen molecules leads to tolylmethoxyl radicals and O-atoms. Methylbenzyl radicals can combine with OH, CH_3 , HO_2 , and themselves to give methylbenzylalcohol, ethyltoluene, methylbenzylhydroperoxide, and bi-methylbenzyl, respectively. The reactions with $\cdot\text{O}$ atoms, which are important at high temperature, lead to tolyl radicals and formaldehyde molecules (32) or to $\cdot\text{H}$ atoms and tolualdehyde molecules (35). Ortho- and para-methylbenzyl radicals can also react by decomposition (30) or with oxygen molecules (32) to form xylylenes. The rate constants of the decomposition by breaking of a C–H bond are those measured by Fernandes et al. [43], and those for the reactions with oxygen are based on the value proposed by Emdee et al. [26] for para-xylene. The activation energy (13.7 kcal/mol) proposed by Emdee et al. is consistent with the enthalpy of reaction which is about 10 kcal/mol at 1000 K. The formation of dihydronaphthalene and methylindene proposed by Marinov et al. [44] by addition to acetylene molecules of ortho-methylbenzyl radicals and meta- or para-methylbenzyl radicals, respectively, has also been taken into account (33).

The reactions of methyl tolyl radicals ((40)–(46)) have been adapted from those proposed for phenyl radi-

cals [11] and includes reactions with oxygen molecules to give $\cdot\text{O}$ atoms and methyl cresoxyl radicals and termination steps with other radicals.

Tolylmethoxyl radicals can react with oxygen to give tolualdehyde and $\cdot\text{HO}_2$ radicals (49), by termination with H-atoms to give methyl benzyl alcohol (50) or by beta-scissions. Two beta-scissions are possible, the first involving the breaking of a C–H bond (47) to give tolualdehyde and H-atoms and the second involving the breaking of a C–C bond (48) to form formaldehyde and methyl phenyl radicals. As in the case of toluene, we have used the same activation energy for both channels.

The reaction of methyl cresoxyl radicals is the same as for cresoxyl radicals, i.e. CO elimination (51,52) and combination with H-atoms yielding methylcresol (53).

Secondary Mechanism

Apart from the additions of H-atoms, which lead to $\cdot\text{CHO}$ radicals and toluene (57) and to benzaldehyde and methyl radicals (58), the reactions of tolualdehyde molecules involve the formation by initiations and by H-abstraction of two resonance-stabilized radicals: methylbenzoyl radicals (formed by reactions (54), (55), (59)–(74)), which decompose to methyl phenyl radicals and carbon monoxide (91), and methoxybenzyl radicals (formed by reactions (56), (74)–(90)), which react according to the main steps of benzyl radicals (reactions (92)–(98)) and lead to the formation of phthaldehyde or benzaldehyde.

Methyl benzyl hydroperoxide molecules can be easily decomposed by rupturing of the O–OH bond (99) with the rate constant proposed for the decomposition of benzyl hydroperoxide molecules [24].

Methyl cresol molecules can react by addition of H-atoms, to give methyl radicals and cresols (102), or by bimolecular initiations ((100) and (101)) and by H-abstraction ((103)–(118) and (119)–(134)) to lead to the formation of two resonance-stabilized radicals, methylcresoxyl and methylhydroxybenzyl radicals,

Table V Primary and Secondary Mechanism for the Oxidation of Xylenes

Reactions	<i>A</i>	<i>n</i>	<i>E_a</i>	References	Reaction No.
PRIMARY MECHANISM					
Reactions of xylene molecules					
<i>Unimolecular initiation</i>					
<i>o</i> -xylene = <i>o</i> -methylbenzyl + H	5.0×10^{15}	0.0	88.3	DaCosta00 [42] ^a	(1)
<i>m</i> -xylene = <i>m</i> -methylbenzyl + H	5.0×10^{15}	0.0	89.7	DaCosta00 [42] ^a	(1)
<i>p</i> -xylene = <i>p</i> -methylbenzyl + H	5.0×10^{15}	0.0	89.0	DaCosta00 [42] ^a	(1)
Xylene = C ₆ H ₄ CH ₃ + CH ₃	4.0×10^{17}	0.0	97.0	Estimated ^b	(2)
<i>Bimolecular initiation</i>					
Xylene + O ₂ = methylbenzyl + HO ₂	4.2×10^{12}	0.0	38.6	Estimated ^c	(3)
<i>Additions</i>					
Xylene + H = toluene + CH ₃	11.6×10^{13}	0.0	8.1	Estimated ^d	(4)
Xylene + O = OC ₆ H ₃ (CH ₃) ₂ + H	1.7×10^{13}	0.0	3.6	Estimated ^e	(5)
Xylene + OH = HOC ₆ H ₃ (CH ₃) ₂ + H	1.3×10^{13}	0.0	10.6	Estimated ^e	(6)
<i>Metatheses</i>					
<i>Metatheses with abstraction of a methyl-benzylic H-atom</i>					
Xylene + R = Methylbenzyl + RH ^f				Estimated ^d	(7–23)
<i>Metatheses with abstraction of a phenylic H-atom</i>					
Xylene + R = Methyltolyl + RH ^h				Estimated ^g	(24–28)
Reactions of methylbenzyl radicals					
<i>Decompositions by beta-scission</i>					
Methylbenzyl => C ₆ H ₆ + H + C ₂ H ₂	6.0×10^{13}	0.0	70.0	Estimated ^e	(29)
<i>o</i> -Methylbenzyl = <i>o</i> -xylylene + H	5.0×10^{15}	0.0	74.2	Fernandes02 [43]	(30)
<i>p</i> -Methylbenzyl = <i>p</i> -xylylene + H	5.0×10^{15}	0.0	70.6	Fernandes02 [43]	(30)
<i>Reactions with oxygen molecules</i>					
Methylbenzyl + O ₂ = CH ₃ C ₆ H ₄ CH ₂ O + O	6.3×10^{12}	0.0	40.0	Estimated ^e	(31)
<i>o</i> -Methylbenzyl + O ₂ => <i>o</i> -xylylene + HO ₂	3.6×10^{13}	0.0	16.7	Estimated ⁱ	(32)
<i>p</i> -Methylbenzyl + O ₂ => <i>p</i> -xylylene + HO ₂	3.6×10^{13}	0.0	13.7	Emdee91 [26]	(32)
<i>Addition reactions</i>					
<i>o</i> -Methylbenzyl + C ₂ H ₂ => C ₁₀ H ₁₀ + H	3.2×10^{11}	0.0	7.0	Marinov96 [44]	(33)
<i>m</i> -Methylbenzyl + C ₂ H ₂ => Methylindene + H	3.2×10^{11}	0.0	7.0	Marinov96	(33)
<i>p</i> -Methylbenzyl + C ₂ H ₂ => Methylindene + H	3.2×10^{11}	0.0	7.0	Marinov96	(33)
<i>Termination reactions</i>					
Methylbenzyl + O = Toly + HCHO	3.5×10^{13}	0.0	0.0	Estimated ^e	(34)
Methylbenzyl + O = CH ₃ C ₆ H ₄ CHO + H	1.0×10^{14}	0.0	0.0	Estimated ^e	(35)
Methylbenzyl + OH = CH ₃ C ₆ H ₄ CH ₂ OH	2.0×10^{13}	0.0	0.0	Estimated ^e	(36)
Methylbenzyl + HO ₂ = CH ₃ C ₆ H ₄ CH ₂ OOH	5.0×10^{12}	0.0	0.0	Estimated ^e	(37)
etC ₆ H ₄ CH ₃ = Methylbenzyl + CH ₃	6.1×10^{15}	0.0	75.1	Estimated ^e	(38)
2Methylbenzyl = Bimethylbenzyl	2.5×10^{11}	0.4	0.0	Estimated ^e	(39)
Reactions of methyltolyl radicals					
<i>Reactions with oxygen molecule</i>					
Methyltolyl + O ₂ = OC ₆ H ₄ (CH ₃) ₂ + O	2.6×10^{13}	0.0	6.1	Estimated ^e	(40)
<i>Termination reactions</i>					
Methyltolyl + H = Xylene	1.0×10^{14}	0.0	0.0	Estimated ^e	(41)
Methyltolyl + H = Methylbenzyl + H	2.0×10^{13}	0.0	0.0	Estimated ^d	(42)
Methyltolyl + O = OC ₆ H ₃ (CH ₃) ₂	1.0×10^{14}	0.0	0.0	Estimated ^e	(43)
Methyltolyl + OH = HOC ₆ H ₄ (CH ₃) ₂	1.0×10^{13}	0.0	0.0	Estimated ^e	(44)
Methyltolyl + CH ₃ = Mesitylene	1.2×10^6	1.96	−3.7	Estimated ^e	(45)
Methyltolyl + HO ₂ = OC ₆ H ₃ (CH ₃) ₂ + OH	5.0×10^{12}	0.0	0.0	Estimated ^e	(46)

Continued

Table V Continued

Reactions	<i>A</i>	<i>n</i>	<i>E_a</i>	References	Reaction No.
Reactions of tolylmethoxyl radicals					
<i>Decomposition by beta-scission</i>					
$\text{CH}_3\text{C}_6\text{H}_4\text{CH}_2\text{O} = \text{H} + \text{CH}_3\text{C}_6\text{H}_4\text{CHO}$	2.0×10^{13}	0.0	27.5	Estimated ^e	(47)
$\text{CH}_3\text{C}_6\text{H}_4\text{CH}_2\text{O} = \text{C}_6\text{H}_4\text{CH}_3 + \text{HCHO}$	2.0×10^{13}	0.0	27.5	Estimated ^e	(48)
<i>Reactions with oxygen</i>					
$\text{CH}_3\text{C}_6\text{H}_4\text{CH}_2\text{O} + \text{O}_2 = \text{HO}_2 + \text{CH}_3\text{C}_6\text{H}_4\text{CHO}$	6.0×10^{10}	0.0	1.6	Estimated ^e	(49)
<i>Termination reactions</i>					
$\text{CH}_3\text{C}_6\text{H}_4\text{CH}_2\text{O} + \text{H} = \text{CH}_3\text{C}_6\text{H}_4\text{CH}_2\text{OH}$	1.0×10^{14}	0.0	0.0	Estimated ^j	(50)
Reactions of methylcresoxyl radicals					
<i>CO elimination with rearrangement</i>					
$\text{OC}_6\text{H}_3(\text{CH}_3)_2 = \text{H} + \text{toluene} + \text{CO}$	3.0×10^{11}	0.0	43.8	Estimated ^e	(51)
$\text{OC}_6\text{H}_3(\text{CH}_3)_2 = \text{CH}_3 + \text{Benzene} + \text{CO}$	3.0×10^{11}	0.0	43.8	Estimated ^e	(52)
<i>Termination reactions</i>					
$\text{OC}_6\text{H}_3(\text{CH}_3)_2 + \text{H} = \text{HOC}_6\text{H}_3(\text{CH}_3)_2$	1.0×10^{14}	0.0	0.0	Estimated ^e	(53)
SECONDARY MECHANISM					
Reactions of tolualdehyde molecules and derived radicals					
$\text{CH}_3\text{C}_6\text{H}_4\text{CHO} = \text{CH}_3\text{C}_6\text{H}_4\text{CO} + \text{H}$	4.0×10^{15}	0.0	83.7	Estimated ^e	(54)
$\text{CH}_3\text{C}_6\text{H}_4\text{CHO} + \text{O}_2 = \text{CH}_3\text{C}_6\text{H}_4\text{CO} + \text{HO}_2$	7.0×10^{11}	0.0	39.5	Estimated ^c	(55)
$\text{CH}_3\text{C}_6\text{H}_4\text{CHO} + \text{O}_2 = \text{CH}_2\text{C}_6\text{H}_4\text{CHO} + \text{HO}_2$	2.1×10^{12}	0.0	41.0	Estimated ^c	(56)
$\text{CH}_3\text{C}_6\text{H}_4\text{CHO} + \text{H} = \text{Toluene} + \text{CHO}$	5.8×10^{13}	0.0	8.1	Estimated ^e	(57)
$\text{CH}_3\text{C}_6\text{H}_4\text{CHO} + \text{H} = \text{C}_6\text{H}_5\text{CHO} + \text{CH}_3$	5.8×10^{13}	0.0	8.1	Estimated ^k	(58)
$\text{CH}_3\text{C}_6\text{H}_4\text{CHO} + \text{R} = \text{CH}_3\text{C}_6\text{H}_4\text{CO} + \text{RH}$				Estimated ^e	(59–74)
$\text{CH}_3\text{C}_6\text{H}_4\text{CHO} + \text{R} = \text{CH}_2\text{C}_6\text{H}_4\text{CHO} + \text{RH}^l$				Estimated ^k	(75–90)
$\text{CH}_3\text{C}_6\text{H}_4\text{CO} = \text{C}_6\text{H}_4\text{CH}_3 + \text{CO}$	4.0×10^{14}	0.0	29.5	Estimated ^e	(91)
$\text{CH}_2\text{C}_6\text{H}_4\text{CHO} + \text{O}_2 = \text{CH}_2\text{OC}_6\text{H}_4\text{CHO} + \text{O}$	6.3×10^{12}	0.0	40.0	Estimated ^k	(92)
$\text{CH}_2\text{C}_6\text{H}_4\text{CHO} + \text{H} = \text{CH}_3\text{C}_6\text{H}_4\text{CHO}$	1.0×10^{14}	0.0	0.0	Estimated ^k	(93)
$\text{CH}_2\text{C}_6\text{H}_4\text{CHO} + \text{HO}_2 = \text{CH}_2\text{OC}_6\text{H}_4\text{CHO} + \text{OH}$	5.0×10^{12}	0.0	0.0	Estimated ^k	(94)
$\text{CH}_2\text{C}_6\text{H}_4\text{CHO} + \text{CH}_3 = \text{C}_6\text{H}_5\text{CHO} + \text{C}_2\text{H}_4$	5.0×10^{12}	0.0	0.0	Estimated ^k	(95)
$\text{CH}_2\text{OC}_6\text{H}_4\text{CHO} \Rightarrow \text{H} + \text{C}_6\text{H}_4(\text{CHO})_2$	2.0×10^{13}	0.0	27.5	Estimated ^k	(96)
$\text{CH}_2\text{OC}_6\text{H}_4\text{CHO} = \text{C}_6\text{H}_5\text{CHO} + \text{HCO}$	2.0×10^{13}	0.0	27.5	Estimated ^k	(97)
$\text{CH}_2\text{OC}_6\text{H}_4\text{CHO} + \text{O}_2 \Rightarrow \text{OOH} + \text{C}_6\text{H}_4(\text{CHO})_2$	6.0×10^{10}	0.0	1.6	Estimated ^k	(98)
Reactions of methylbenzyl hydroperoxide molecules					
$\text{C}_6\text{H}_5\text{CH}_2\text{OOH} = \text{C}_6\text{H}_5\text{CH}_2\text{O} + \text{OH}$	1.5×10^{16}	0.0	42.0	Estimated ^e	(99)
Reactions of methylcresol molecules and derived radicals					
$\text{HOC}_6\text{H}_3(\text{CH}_3)_2 + \text{O}_2 = \text{OC}_6\text{H}_3(\text{CH}_3)_2 + \text{HO}_2$	1.0×10^{13}	0.0	38.9	Estimated ^c	(100)
$\text{HOC}_6\text{H}_3(\text{CH}_3)_2 + \text{O}_2 = \text{HOC}_6\text{H}_3\text{CH}_3\text{CH}_2 + \text{HO}_2$	2.1×10^{12}	0.0	39.7	Estimated ^c	(101)
$\text{HOC}_6\text{H}_3(\text{CH}_3)_2 + \text{H} = \text{HOC}_6\text{H}_4\text{CH}_3 + \text{CH}_3$	5.8×10^{13}	0.0	8.1	Estimated ^e	(102)
$\text{HOC}_6\text{H}_3(\text{CH}_3)_2 + \text{R} = \text{OC}_6\text{H}_3(\text{CH}_3)_2 + \text{RH}$				Estimated ^e	(103–118)
$\text{HOC}_6\text{H}_3(\text{CH}_3)_2 + \text{R} = \text{HOC}_6\text{H}_3\text{CH}_3\text{CH}_2 + \text{RH}^l$				Estimated ^d	(119–134)
$\text{HOC}_6\text{H}_3\text{CH}_3\text{CH}_2 + \text{O}_2 = \text{HOC}_6\text{H}_3\text{CH}_3\text{CH}_2\text{O} + \text{O}$	6.3×10^{12}	0.0	40.0	Estimated ^k	(135)
$\text{HOC}_6\text{H}_3\text{CH}_3\text{CH}_2 + \text{H} = \text{HOC}_6\text{H}_3(\text{CH}_3)_2$	1.0×10^{14}	0.0	0.0	Estimated ^k	(136)
$\text{HOC}_6\text{H}_3\text{CH}_3\text{CH}_2 + \text{HO}_2 = \text{HOC}_6\text{H}_3\text{CH}_3\text{CH}_2\text{O} + \text{OH}$	5.0×10^{12}	0.0	0.0	Estimated ^k	(137)
$\text{HOC}_6\text{H}_3\text{CH}_3\text{CH}_2 + \text{CH}_3 = \text{HOC}_6\text{H}_4\text{CH}_3 + \text{C}_2\text{H}_4$	5.0×10^{12}	0.0	0.0	Estimated ^k	(138)
$\text{HOC}_6\text{H}_3\text{CH}_3\text{CH}_2\text{O} = \text{H} + \text{HOC}_6\text{H}_3\text{CH}_3\text{CHO}$	2.0×10^{13}	0.0	27.5	Estimated ^k	(139)
$\text{HOC}_6\text{H}_3\text{CH}_3\text{CH}_2\text{O} = \text{OC}_6\text{H}_4\text{CH}_3 + \text{HCHO}$	2.0×10^{13}	0.0	27.5	Estimated ^k	(140)
$\text{HOC}_6\text{H}_3\text{CH}_3\text{CH}_2\text{O} + \text{O}_2 = \text{HO}_2 + \text{HOC}_6\text{H}_3\text{CH}_3\text{CHO}$	6.0×10^{10}	0.0	1.6	Estimated ^k	(141)
$\text{HOC}_6\text{H}_3\text{CH}_3\text{CHO} + \text{R} = \text{HOC}_6\text{H}_3\text{CH}_3\text{CO} + \text{RH}^l$	4.0×10^{13}	0.0	3.2	Estimated ^k	(142–146)
$\text{HOC}_6\text{H}_3\text{CH}_3\text{CO} = \text{OC}_6\text{H}_4\text{CH}_3 + \text{CO}$	4.0×10^{14}	0.0	29.5	Estimated ^e	(147)
Reactions of methylbenzylalcohol molecules and derived radicals					
$\text{CH}_3\text{C}_6\text{H}_4\text{CH}_2\text{OH} + \text{O}_2 = \text{HO}_2 + \text{CH}_3\text{C}_6\text{H}_4\text{CHOH}$	1.4×10^{12}	0.0	34.0	Estimated ^c	(148)
$\text{CH}_3\text{C}_6\text{H}_4\text{CH}_2\text{OH} + \text{H} = \text{Toluene} + \text{CH}_2\text{OH}$	5.8×10^{13}	0.0	8.1	Estimated ^e	(149)

Continued

Table V Continued

Reactions	<i>A</i>	<i>n</i>	<i>E_a</i>	References	Reaction No.
CH ₃ C ₆ H ₄ CH ₂ OH + H = CH ₃ + C ₆ H ₅ CH ₂ OH	5.8 × 10 ¹³	0.0	8.1	Estimated ^k	(150)
CH ₃ C ₆ H ₄ CH ₂ OH + R = RH + CH ₃ C ₆ H ₄ CHOH ^l				Estimated ^e	(151–166)
CH ₃ C ₆ H ₄ CHOH = CH ₃ C ₆ H ₄ CHO + H	2.0 × 10 ¹⁴	0.0	23.3	Estimated ^e	(167)
Reactions of ethyltoluene molecules and derived radicals					
etC ₆ H ₄ CH ₃ = CH ₃ CHC ₆ H ₄ CH ₃ + H	4.3 × 10 ¹⁴	0.0	83.6	Estimated ^e	(168)
etC ₆ H ₄ CH ₃ + O ₂ = CH ₃ CHC ₆ H ₄ CH ₃ + HO ₂	1.4 × 10 ¹²	0.0	34.0	Estimated ^c	(169)
etC ₆ H ₄ CH ₃ + H = Toluene + C ₂ H ₅	5.8 × 10 ¹³	0.0	8.1	Estimated ^e	(170)
etC ₆ H ₄ CH ₃ + H = etC ₆ H ₅ + CH ₃	5.8 × 10 ¹³	0.0	8.1	Estimated ^e	(171)
etC ₆ H ₄ CH ₃ + R = CH ₃ CHC ₆ H ₄ CH ₃ + RH ^l				Estimated ^e	(172–187)
CH ₃ CHC ₆ H ₄ CH ₃ = H + Methylstyrene	3.1 × 10 ¹³	0.0	50.7	Estimated ^e	(188)
CH ₃ CHC ₆ H ₄ CH ₃ + O ₂ = HO ₂ + Methylstyrene	7.0 × 10 ¹¹	0.0	15.0	Estimated ^e	(189)
CH ₃ CHC ₆ H ₄ CH ₃ + HO ₂ = OH + CH ₃ C ₆ H ₄ CHO + CH ₃	5.0 × 10 ¹²	0.0	0.0	Estimated ^e	(190)
Reactions of bimethylbenzyl molecules and derived radicals					
Bimethylbenzyl = C ₁₆ H ₁₇ + H	1.0 × 10 ¹⁴	0.0	83.0	Estimated ^e	(191)
Bimethylbenzyl + O ₂ = C ₁₆ H ₁₇ + HO ₂	2.8 × 10 ¹²	0.0	35.0	Estimated ^e	(192)
Bimethylbenzyl + R = C ₁₆ H ₁₇ + RH ^l				Estimated ^e	(193–208)
C ₁₆ H ₁₇ = Dimethylstilbene + H	7.1 × 10 ¹⁴	0.0	30.0	Estimated ^e	(209)
Reactions of xylylene molecules and derived compounds (only for ortho- or para-xylene)					
<i>o</i> -xylylene = Benzocyclobutene	2.1 × 10 ¹²	0.0	26.8	Roth81[45]	(210)
Benzocyclobutene = Styrene	1.2 × 10 ¹⁵	0.0	74.3	Tsang90[46]	(211)
<i>o</i> -Xylylene + O = <i>o</i> -CH ₂ C ₆ H ₄ CHO + H	6.0 × 10 ⁸	1.45	0.9	Estimated ^m	(212)
<i>p</i> -Xylylene + O = <i>o</i> -CH ₂ C ₆ H ₄ CHO + H	6.0 × 10 ⁸	1.45	0.9	Estimated ^m	(212)
Reactions of dihydronaphthalene molecules and derived compounds (only for ortho-xylene)					
C ₁₀ H ₁₀ + OH = C ₁₀ H ₉ + H ₂ O	5.0 × 10 ⁶	2.0	0.0	Marinov96	(213)
C ₁₀ H ₁₀ + H = C ₁₀ H ₉ + H ₂	2.0 × 10 ⁵	2.5	2.5	Marinov96	(214)
C ₁₀ H ₁₀ + O = C ₁₀ H ₉ + OH	7.0 × 10 ¹¹	0.7	6.0	Marinov96	(215)
Naphthalene + H = C ₁₀ H ₉	5.0 × 10 ¹⁴	0.0	5.0	Marinov96	(216)

The rate constants are given at 1 atm ($k = AT^n \exp(-E_a/RT)$) in cc, mol, s, kcal units. Reference numbers are given in brackets when they appear for the first time. This mechanism should be used together with the mechanism for the oxidation of benzene [11] and toluene [24]. When the type of isomer is not specified, the reaction considered in the mechanism for each of the three compounds.

^a The *A* factor has been divided by 2.

^b Rate constant taken equal to that proposed for toluene [24] multiplied by 4.

^c The rate constant of this bimolecular initiation with oxygen molecule has been calculated as proposed by Ingham et al. [47]: *A* is taken equal to $n \times 7 \times 10^{11} \text{ cm}^3 \text{ mol}^{-1} \text{ s}^{-1}$, where *n* is the number of benzylic hydrogen atoms abstractable, and the activation energy to the reaction enthalpy.

^d Rate constant is taken equal to that of the similar reaction in the mechanism of the oxidation of toluene [24] multiplied by 2 to take into account the number of abstractable H-atoms or of methyl groups.

^e Rate constant is taken equal to that of the similar reaction in the mechanism of the oxidation of toluene [24].

^f Where R is H, O, OH, HO₂, CH₃, C₂H₃, C₃H₅, C₃H₃, *i*-C₄H₅, *n*-C₄H₅, cyclopentadienyl, phenyl, phenoxy, benzyl, cresoxy, tolyl, methylcresoxy radicals.

^g Rate constant is taken equal to that proposed for benzene [11] multiplied by 2.

^h Where R is H, O, OH, HO₂, CH₃ radicals.

ⁱ Rate constant is deduced from that of the similar reaction in the case of *p*-xylene and the difference in enthalpies of formation between the ortho and para isomers of xylylene [41].

^j Rate constant is taken equal to that of the recombination of •H atoms with alkyl radicals as proposed by Allara et al. [48].

^k Rate constant is taken equal to that of the similar reaction in the case of benzyl radicals and derived species [24].

^l Where R is H, O, OH, HO₂, CH₃, C₂H₅, C₃H₅, C₃H₃, *i*-C₄H₅, *n*-C₄H₅, cyclopentadienyl, phenoxy, benzyl, cresoxy, methylbenzyl, OC₆H₄(CH₃)₂ radicals.

^m Rate constant is taken equal to that of the similar reaction in the case of 1,3-butadiene [33].

respectively. The reactions deriving from methylhydroxybenzyl radicals ((135)–(147)) are deduced from the major steps deriving from benzyl radicals.

Apart from the additions of H-atoms, which lead to CH₂OH radicals and toluene (149) or to methyl

radicals and benzyl alcohol (150), the reactions of methylbenzylalcohol molecules involve the formation of the resonance stabilized tolylmethylhydroxyl radicals by bimolecular initiation (148) and by H-abstraction ((151)–(166)). The formation of the

other possible radicals with a higher energy of formation has been neglected. Tolylmethylhydroxyl radicals can decompose to hydrogen atoms and tolualdehyde (167).

In the case of ethyltoluene molecules, the additions of H-atoms lead to C_2H_5 radicals and toluene (170) or to ethylbenzene and methyl radicals (171). Unimolecular (168), bimolecular initiation (169), and H-abstraction ((172)–(187)) involve the formation of the resonance stabilized tolylethyl radicals; the formation of the other possible radicals has been neglected, because they are not resonance stabilized. Tolylethyl radicals lead to the formation of methylstyrene by decompositions involving the breaking of a C–H bond (188) or by reaction with oxygen molecules (189) or combine with HO_2 radicals (190) to give hydroperoxide molecules, which quickly decompose.

In the case of bimethylbenzyl molecules, we have only considered the formation of the resonance stabilized ditolylethyl radicals by unimolecular (191) and bimolecular (192) initiation and by H-abstraction ((193)–(208)). Ditolylethyl radicals can decompose to give hydrogen atoms and dimethylstilbene (209).

The reactions of xylenes have not been much investigated previously. We consider that they can react with O-atoms to give methoxybenzyl radicals (212). Roth and Scholz [45] have studied the isomerization of *o*-xylene to give benzocyclobutene (210) and proposed a rate constant that we have used. Benzocyclobutene leads to styrene (211) with a rate constant proposed by Tsang and Cui [46].

Dihydronaphthalene leads to naphthalene through H-abstraction by H and O atoms and OH radicals ((213)–(215)) and beta-scission involving the breaking of a C–H bond (216).

COMPARISON BETWEEN COMPUTED AND EXPERIMENTAL RESULTS

Simulations were performed using the CHEMKIN II software [32]. We have tried to reproduce our experimental data obtained in a shock tube, but to extend the validity of the proposed mechanism, we have also attempted to model results of the literature obtained in a flow tube [25,26].

Shock Tubes

Computed results for our shock tube appear in Figs. 1–4. It is worth noting that the experimental OH emission at 306 nm is related to the electronically excited OH^* population and is not directly proportional to OH radical concentration. Nevertheless, previous work [33] has shown a correct agreement between the shapes

of the profiles of experimental emission and calculated OH concentration during the rise of the signal, which is the important part of the curve for the determination of ignition delays. Both experimentally and theoretically, the ignition delay is determined at 10% of the maximum OH peak. Simulations reproduce the systematic trends of the measurements, including variations in ignition delay times with temperature, equivalence ratio, and concentration of hydrocarbon and that for the three isomers of xylenes. Simulations shown in Fig. 4 reproduce well the fact that these three compounds have a very similar reactivity under these conditions.

Flow Reactor

Emdee et al. [25,26] have studied the oxidation of the three isomers of xylene in a flow reactor at ~ 1150 K, at atmospheric pressure, with nitrogen as bath gas, for an initial concentration of xylene from 1400 to 1700 ppm and for equivalence ratios from 0.47 to 1.7.

Figures 5–7 display comparisons between the experimental and computed mole fraction of reactants and

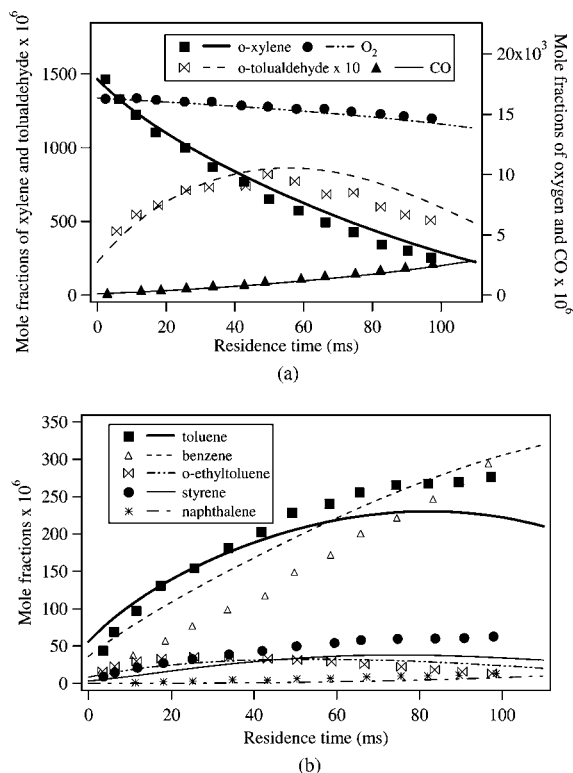
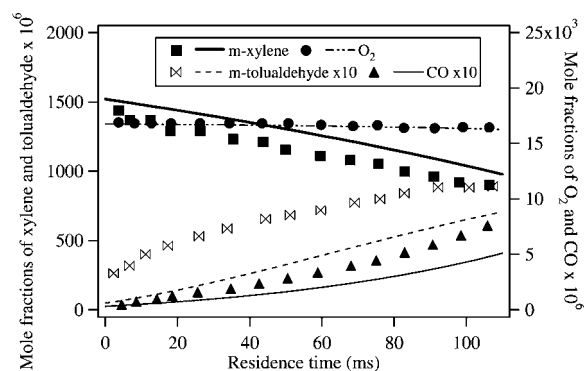
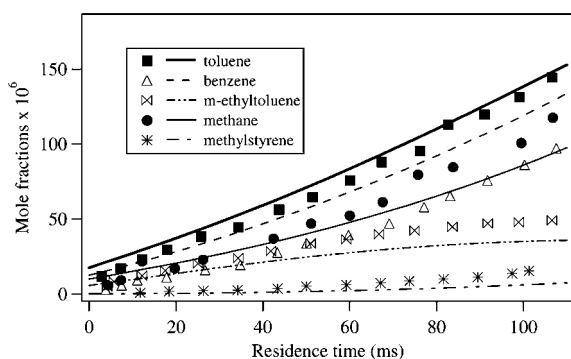


Figure 5 Oxidation of *o*-xylene in a flow reactor at 1150 K, $P = 1$ atm, and $\Phi = 1.1$, with an initial concentration of hydrocarbon of 1700 ppm [26]. Comparison between experimental (symbols) and computed (lines) species mole fractions versus residence time with simulated time –10 ms shifted.



(a)

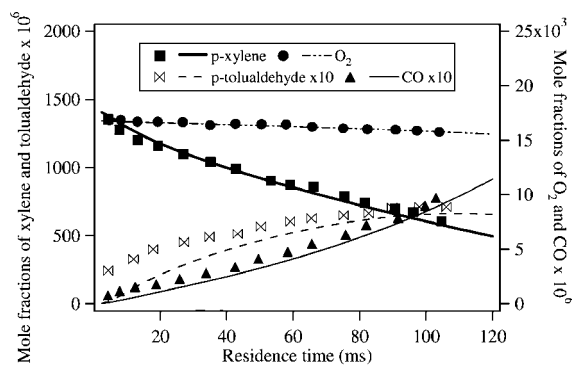


(b)

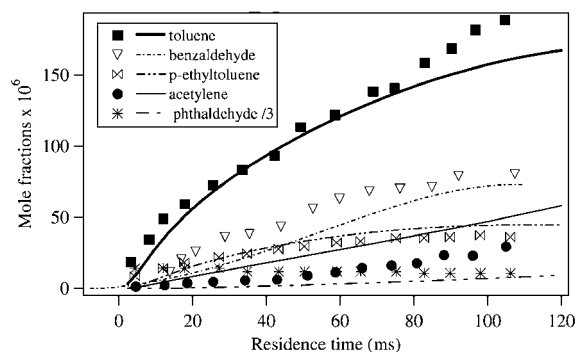
Figure 6 Oxidation of *m*-xylene in a flow reactor at 1155 K, $P = 1$ atm and $\Phi = 1.0$, with an initial concentration of hydrocarbon of 1580 ppm [26]. Comparison between experimental (symbols) and computed (lines) species mole fractions versus residence time with simulated time ~ 20 ms shifted.

main products for the three xylenes for stoichiometric mixtures. These figures show that a globally correct agreement can be observed. The consumption of hydrocarbon and oxygen (Figs. 5a, 6a, 7a) is correctly reproduced, even if that of meta-xylene is slightly underestimated. The formation of major products, tolualdehyde (Figs. 5a, 6a, 7a), ethyl-toluene (Figs. 5b, 6b, 7b), phthaldehyde (Fig. 7b), methyl styrene (Fig. 6b), toluene (Figs. 5b, 6b, 7b), benzaldehyde (Fig. 7b), benzene (Figs. 5b and 6b), carbon monoxide (Figs. 5a, 6a, 7a), methane (Fig. 6b), and acetylene (Fig. 7b) is also globally well captured by the simulations. In the case of ortho-xylene, the formation of styrene and naphthalene (Fig. 5b), which is specific to this compound, is correctly simulated.

Figure 8 displays a comparison between the conversion of the three xylenes and shows that the proposed models correctly reproduce the difference of reactivity between these three compounds. Ortho-xylene is much more reactive than meta- and para-xylenes, while para-xylene is slightly more reactive than meta-xylene. A comparison with the conversion of toluene



(a)



(b)

Figure 7 Oxidation of *p*-xylene in a flow reactor at 1155 K, $P = 1$ atm and $\Phi = 0.89$, with an initial concentration of hydrocarbon of 1420 ppm [26]. Comparison between experimental (symbols) and computed (lines) species mole fractions versus residence time.

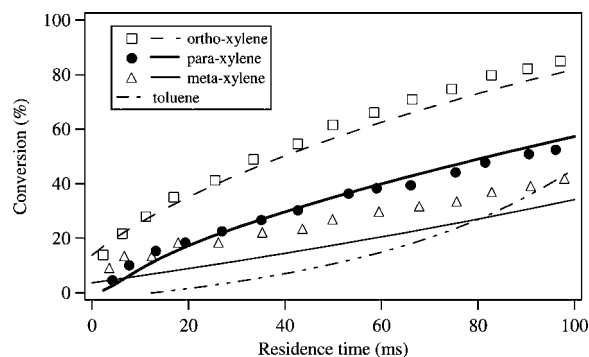


Figure 8 Comparison between the conversions of the three xylenes and toluene in a flow reactor at 1155 K, $P = 1$ atm and Φ close to 1 [26]. Experimental (symbols) and computed (lines) conversions (only simulations for toluene) versus residence time under the same conditions as in Figs. 5–7. Calculations have been performed for toluene under the same conditions as for para-xylene. The same time shifts as in Figs. 5 and 6 have been used.

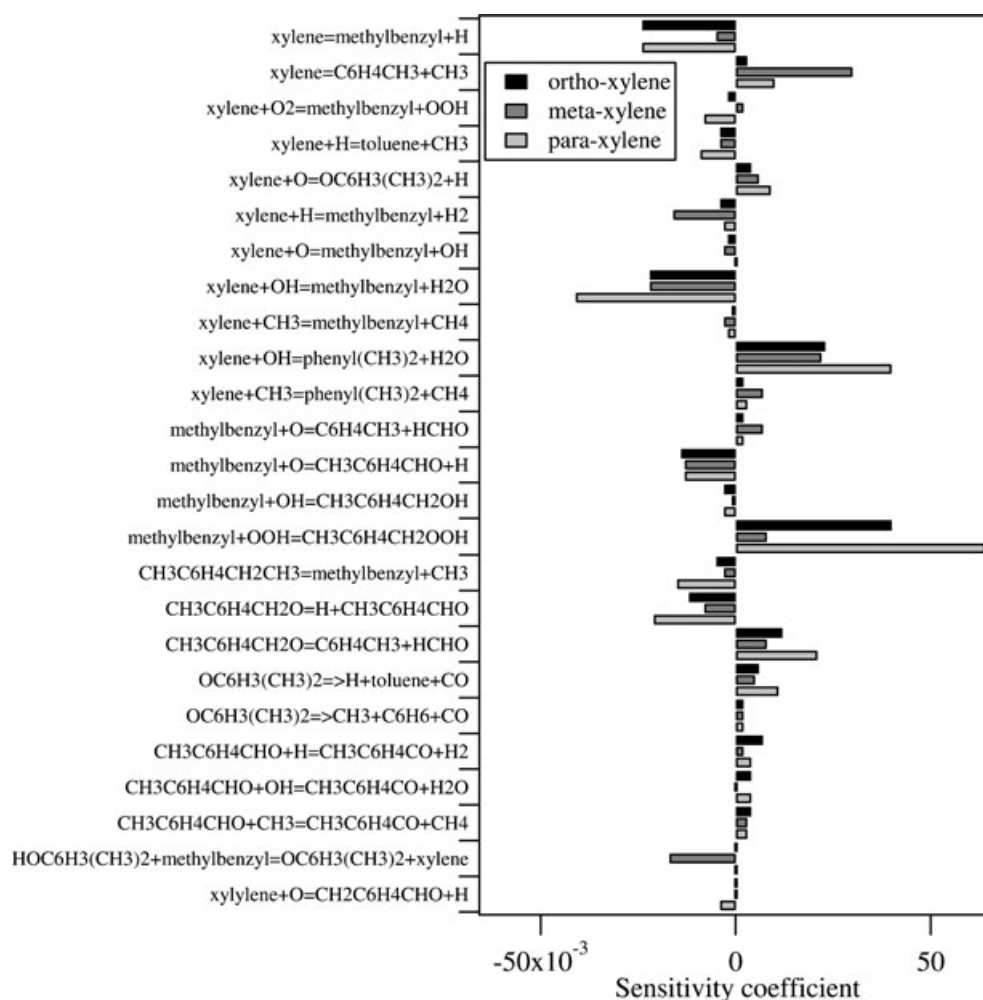


Figure 9 Sensitivity analyses related to the mole fraction of CO in a flow reactor at 1155 K, $P = 1$ atm, $\Phi = 1.1$, and a residence time of 0.02 s. (For the clarity of the figure, only reactions of Table V with an absolute value of the normalized sensitivity coefficient above 0.003 are shown.)

computed under the same conditions as para-xylene shows that the monosubstituted compound is much less reactive for residence time below 40 ms and has a reactivity close to that of meta-xylene for larger residence times.

ANALYSIS OF THE MECHANISM AND DISCUSSION

The flow and sensitivity analyses presented hereafter have been performed with the three mechanisms described previously. The accuracy of conclusions derived from them can only reflect the accuracy of the proposed reaction channels and of the used thermodynamic and kinetic data.

Figures 9 and 10 present sensitivity and flow analyses, respectively, computed in a flow reactor at 1155 K. Sensitivity analyses have been performed to know the

effect of a variation of a given rate constant on the mole fraction of carbon monoxide. A positive coefficient indicates that the related reaction has a promoting effect. Sensitivity analyses are displayed for the three xylenes, but this flow analysis is only shown for ortho-xylene, as this isomer involves the highest numbers of reaction pathways including all those which are common to the three species. These analyses have been performed at the same residence time corresponding to a conversion of 36% for ortho-xylene, 9.5% for meta-xylene, and 18% for para-xylene.

Figures 11 and 12 present sensitivity and flow analyses, respectively, computed in a shock tube. The analysis displayed in Fig. 11 is for meta-xylene and shows the influence of the most sensitive reactions consuming xylene. Figure 11 also presents a comparison with toluene for a mixture with a close composition ($\Phi = 1$, 0.5% toluene compared to 0.625% of xylene) and shows that this monosubstituted aromatic species is much less

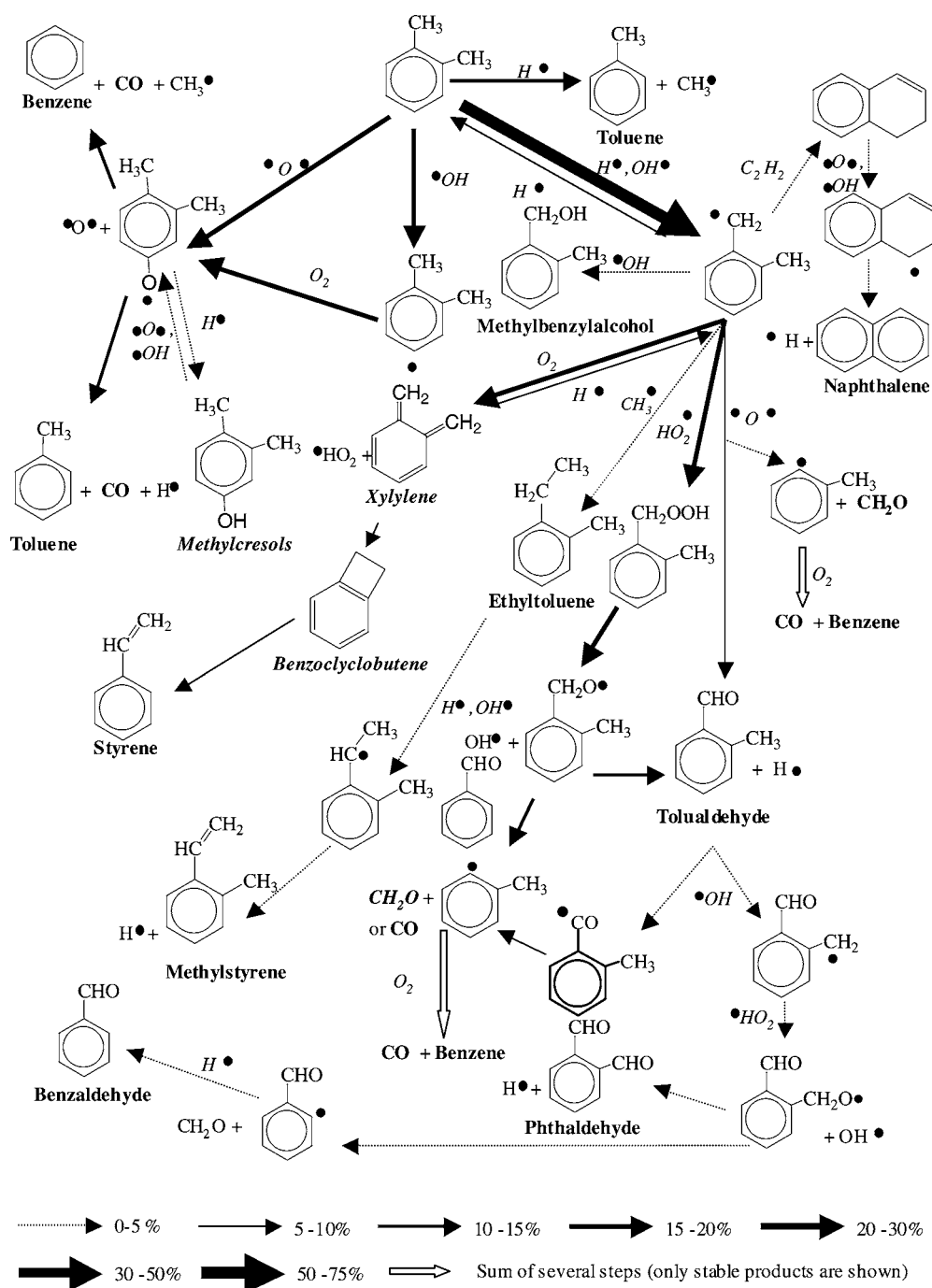


Figure 10 Flow analysis related to the oxidation of ortho-xylene in a flow reactor at 1155 K, $P = 1$ atm, $\Phi = 1.1$, and a residence time of 0.02 s. Products written in *italics* have not been experimentally observed [25].

reactive than xylenes. The flux analysis displayed in Fig. 12 has been computed for para-xylene at 1720 K.

Main Reaction Pathways of Xylene Molecules

Low Temperature. At 1155 K, in flow reactor conditions, whatever the isomers, xylene molecules mainly

react according to four types of reactions in a very similar way compared to toluene:

- ♦ ipso-additions of H-atoms to give methyl radicals and toluene (reaction (4) in Table V, 12% of the consumption for ortho-xylene under the conditions shown in Fig. 10),

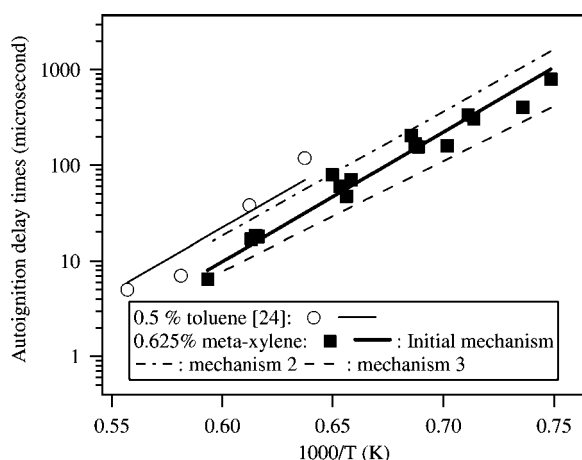


Figure 11 Sensitivity analyses in a shock tube for meta-xylene and comparison with toluene. Semi-log plot of experimental (symbols) and computed (lines) ignition delay times as a function of temperature behind the reflected shock wave at $\Phi = 1$. Mechanisms 2 and 3 have been obtained by dividing by 10 the rate constant of the initiation step (2) and that of the abstraction of benzylic H-atoms by H atoms (7) and OH radicals (9), respectively.

- ♦ abstractions of phenylic H-atoms mainly by OH radicals to give methyltolyl radicals (reactions (24), 13% of the consumption for ortho-xylene), which mostly react with oxygen molecules to form methylcresoxy radicals,
- ♦ ipso-additions of O-atoms to give H-atoms and methylcresoxy radicals (reaction (5), 13% of the consumption for ortho-xylene), which mostly decompose to give carbon monoxide and benzene and methyl radicals or toluene and H-atoms, and
- ♦ abstractions of benzylic H-atoms mainly by H-atoms and OH radicals to give methylbenzyl radicals (reactions (7) and (9), 60% of the consumption for ortho-xylene).

Figure 9 shows that, at 1155 K, the ipso-additions of H-atoms have a slight inhibiting effect as they consume H-atoms to form the less reactive methyl radicals. The sensitivity on the formation of carbon monoxide of the ipso-additions of O-atoms (reaction (5)) is probably enhanced by the fact that methylcresoxy radicals lead mainly to carbon monoxide through reactions (51) and (52). The abstractions of benzylic H-atoms reactions have a strong inhibiting effect as they lead to resonance stabilized methylbenzyl radicals, which react mainly by termination steps. To the contrary, the abstractions of phenylic H-atoms, which directly compete with the previous ones, have a strong promoting effect.

Initiation reactions ((1), (2), or (3)) are also present in the sensitivity analysis shown in Fig. 9, even if

their fluxes of consumption of xylene are negligible, apart from reaction (2) which accounts for 8% of the consumption of meta-xylene and strongly accelerates the oxidation of this species. Reaction (1) exhibits an important negative coefficient because the reverse termination step is dominant.

High Temperature. At 1720 K, whatever the isomers, the flux analysis gives a much different picture: xylene molecules mainly react according to only three types of reactions:

- ♦ ipso-additions of H-atoms to give methyl radicals and toluene (reaction (4), 6% of the consumption for para-xylene under the conditions shown in Fig. 12),
- ♦ abstractions of benzylic H-atoms mainly by H atoms and OH radicals to give methylbenzyl radicals (reactions (7) and (9), 16% of the consumption for para-xylene), and
- ♦ unimolecular initiation to give methyl radicals and tolyl radicals (reaction (2), 75% of the consumption for para-xylene), which mainly react with oxygen molecules to give ultimately carbon monoxide and benzene.

Figure 11 displayed simulations obtained by dividing by 10 the rate constant of the unimolecular initiation (2) showing the strong promoting effect of this reaction at 1720 K. This figure also displays the effect of a division by 10 of the rate constant of the abstraction of benzylic H-atoms by H atoms (7) and OH radicals (9) enlightening the strong inhibiting effect of these reactions. The fact that the rate constant of the unimolecular initiation (1) is larger in the case of xylenes compared to toluene (a factor 6 at 1700 K) mostly explains the lower reactivity of the monosubstituted aromatic compounds shown in Fig. 11. While a study of the fast flow pyrolysis of *p*-xylene between 1200 and 1380 K [50] showed some importance of the H-abstraction between tolyl radicals and xylene, the flow rate of this reaction was found negligible under the conditions shown in Figs. 10 and 12.

Reactions Deriving from the Formation of Methylbenzyl Radicals and Explanation of the Difference of Reactivity between the Three Isomers

Low Temperature. At 1155 K, in flow reactor conditions, as benzyl radicals, the three isomers of methylbenzyl radicals react mainly by termination steps with H-atoms (reaction (1)), O-atoms (reactions (34) and (35)), and OH (reaction (36)), methyl (reaction (38)),

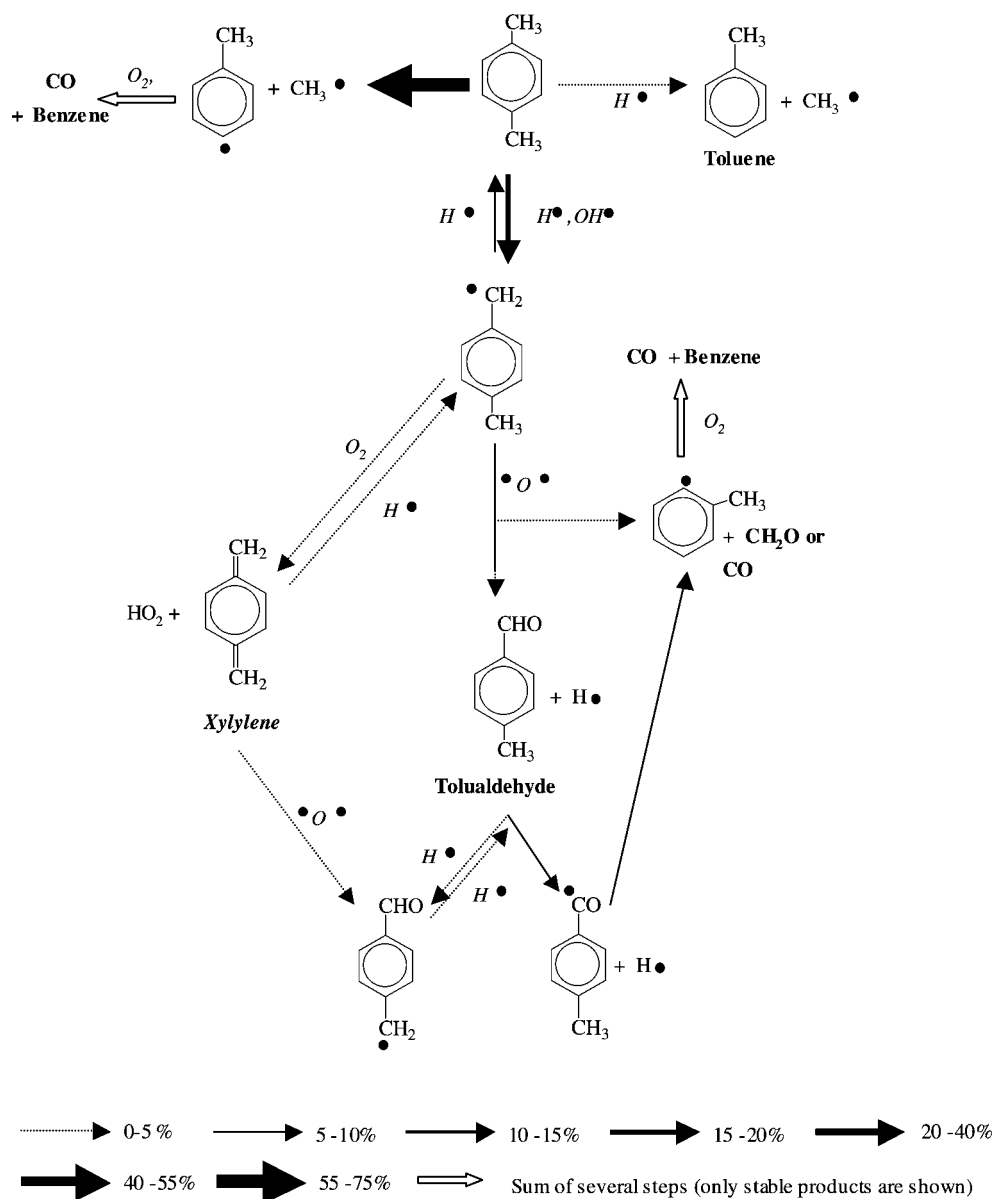


Figure 12 Flow analysis related to the oxidation of para-xylene in a shock tube at 1720 K, $P = 7.8$ atm, $\Phi = 1$, and a residence time of 9.5 μs corresponding to the autoignition start.

and HO_2 (reaction (37)) radicals. The termination reactions with H-atoms, OH, and methyl radicals form, respectively, xylene, methyl benzylalcohol, and ethyl-toluene, which leads to methylstyrene, and have a slight inhibiting effect. A small fraction of the reaction with O-atoms leads to tolyl radicals (reaction (34)), which react with oxygen molecules through a branching step to give methylphenoxy radicals and O-atoms. That explains the promoting effect of this reaction and the inhibiting one of the directly competing channel producing tolualdehyde and H-atoms (reaction (35)). The termination steps with $HO_2\cdot$ radicals have a strong promoting effect as they form a hydroperoxide which al-

most immediately decomposes to give OH and tolyl-methoxyl radicals (reaction (99)). These last radicals in turn decompose to produce formaldehyde and tolyl radicals (reaction (48)) or H-atoms and tolualdehyde (reaction (47)). Tolualdehyde can react by abstraction by OH radicals of either a benzylic H-atom (reaction (77)) to lead to benzaldehyde and formaldehyde or to phthaldehyde or a aldehydic H-atom (reaction (61)) to involve the formation of benzene and carbon monoxide.

In the case of meta-methylbenzyl radicals, these termination steps are the only possible reactions and that explains the very low reactivity of meta-xylene, especially as the consumption of H-atoms by the

termination step with methylbenzyl radicals has a higher flow rate than that by branching step with oxygen molecules. In the case of ortho- and para- methylbenzyl radicals, the formation of xylene by reaction with oxygen molecules (reaction (32)) is possible and has an important flux (20% of the consumption of xylene). This reaction increases the concentration of HO₂ radicals, which is more than 10 times larger in the case of ortho- and para-xylene than for the meta-isomer in the same conditions. This step favors the formation of methylbenzyl hydroperoxide and promotes the global reactivity of ortho- and para-xylene as shown in Fig. 8.

In summary, the reactions of meta-xylene are very similar to that of toluene, which explains why both compounds have a close reactivity for residence times above 40 ms in a flow reactor, as shown in Fig. 8. Nevertheless, as the reversible recombinations of benzyl radicals with themselves ($\Delta H_r(298\text{ K}) = -64.1\text{ kcal/mol}$) are thermodynamically favored compared to that of methylbenzyl radicals (reaction (39)) ($\Delta H_r(298\text{ K}) = -49.2\text{ kcal/mol}$), their fluxes are larger for toluene (13.5% of the consumption benzyl radicals under the same conditions as in Fig. 10) than for xylenes (0.04% of the consumption methylbenzyl radicals for meta-xylene). That explains why the conversion of toluene is much lower for low residence times, before an equilibrium bibenzyl concentration is reached.

Ortho-xylene is consumed for around 50% by addition of H-atoms to give back methylbenzyl radicals (reaction (-30)) and for 50% by isomerization to give benzocyclobutene (reaction (210)) and then styrene (reaction (211)); while para-xylene is 80% consumed by addition of H-atoms to give back methylbenzyl radicals and only 20% by reaction with O-atoms to give H-atoms and methoxybenzyl radicals (reaction (212)). The consumption of H-atoms to give back the resonance stabilized methylbenzyl radicals decreases the global reactivity, and the absence of possible concurrent isomerization in the case of para-xylene explains then why it is much less reactive than ortho-xylene as shown in Fig. 8.

High Temperature. At 1720 K, methylbenzyl radicals react mainly by termination steps with H-atoms (reaction (-1)) and with O-atoms to give tolualdehyde and H-atoms (reaction (35)). The formation of para-xylene under the conditions shown in Fig. 12 has a very small flux (2% of the consumption of xylene), which explains why there is no difference of reactivity in shock tube experiments, taking into account that the rate constants of the very sensitive initiation reaction (reaction (1)) and abstractions of benzylic H-atoms (reactions (7) and (9)) are the same whatever the isomer.

CONCLUSION

This paper presents new experimental results for the autoignition of the three isomers of xylene in a shock tube between 1300 and 1820 K, showing a similar reactivity for the three compounds. It also proposes a set of detailed mechanisms able to reproduce these data, but also previously published experiments in a flow reactor at 1155 K [25,26] exhibiting important differences of reactivity between the three species. To our knowledge, it is the first attempt of a kinetic-detailed modeling of the three isomers of this bisubstituted aromatic species.

The reactions of importance in these mechanisms have been determined by using flux and sensitivity analyses. That has allowed us to explain the differences of reactivity obtained between the three isomers of xylenes: the possible ways of formation and consumption of xylenes are responsible of the important differences of reactivity observed in a flow reactor at 1155 K, while the dominant importance of initiation reactions with the same rate constant encounters the fact that no difference is obtained in a shock tube between 1300 and 1800 K.

It is worth noting that these mechanisms are mostly based on reactions and rate constants guessed from analogies with toluene and benzene and should certainly be revisited when more experimental data are available. Future work could include the extension of the validity of these mechanisms toward lower temperatures, i.e. below 1000 K, by considering the formation of peroxy radicals, in order to model the results obtained in a rapid compression machine [27,28].

BIBLIOGRAPHY

1. Guibet, J. C. In *Fuels & Engines*, Vols. 1 and 2; Publications de l'Institut Français du Pétrole, Editions Technip, 1999.
2. Emdee, J. L.; Brezinsky, K.; Glassman, I. *J Phys Chem* 1992, 96, 2151–2161.
3. Lindstedt, R. P.; Skevis, G. *Combust Flame* 1994, 99, 551–561.
4. Zhang, H. Y.; McKinnon, J. T. *Combust Sci Technol* 1995, 107, 261.
5. Tan, Y.; Frank, P. *Symp Int Combust Proc* 1996, 26, 677–684.
6. Shandross, R. A.; Longwell, J. P.; Howard, J. B. *Proc Combust Inst* 1996, 26, 711–719.
7. Richter, H.; Grieco, W. J.; Howard, J. *Combust Flame* 1999, 119, 1–22.
8. Alzueta, M. U.; Glarborg, P.; Dam-Johansen, K. *Int J Chem Kinet* 2000, 32, 498–522.
9. Ristori, A.; Dagaut, P.; El Bakali, A.; Pengloan, G.; Cathonnet, M. *Combust Sci Technol* 2001, 167, 223–256.

10. Dupont, L.; El Bakali, A.; Pauwels, J. F.; Da Costa, I.; Meunier, P.; Richter, H. *Combust Flame* 2003, 135, 171–183.
11. Da Costa, I.; Fournet, R.; Billaud, F.; Battin-Leclerc, F. *Int J Chem Kinet* 2003, 35, 503–524.
12. Brezinsky, K.; Litzinger, T. A.; Glassman, I. *Int J Chem Kinet* 1984, 16, 1053–1074.
13. Klotz S. D.; Brezinsky, K.; Glassman, I. *Proc Combust Inst* 1998, 27, 337–344.
14. Dagaut, P.; Pengloan, G.; Ristori, A. *Phys Chem Chem Phys* 2002, 4, 1846–1854.
15. Sivaramakrishnan, R.; Tranter, R. S.; Brezinsky, K.; Durgam, S.; Vasudevan, H. *Proc Combust Inst* 2005, 30, 1165–1173.
16. Burcat, A.; Snyder, C.; Brabbs, T. NASA TM-87312, 1986.
17. Pengloan, G. Ph. D. thesis, Université d'Orléans, 2001.
18. Roubaud, A.; Minetti, R.; Sochet, L.R. *Combust Flame* 2000, 123, 535–541.
19. Hamins, A.; Seshadri, K. *Combust Flame* 1987, 68, 295–307.
20. Davis, S. G.; Wang, H.; Brezinsky, K.; Law C. K. *Proc Combust Inst* 1996, 26, 1025–1033.
21. Lindstedt, R. P.; Maurice, L. Q. *Combust Sci Technol* 1996, 120, 119–167.
22. Pitz, W. J.; Seiser, R.; Bozzelli, J. W.; I. Da Costa, I.; Fournet, R.; Billaud, F.; Battin-Leclerc, F.; Seshadri, K.; Westbrook, C. K. In *Proceedings of the 2nd Joint Meeting of the U.S. Sections of the Combustion Institute*, 2001.
23. Vasudevan, V.; Davidson, D. F.; Hanson, R. K. *Proc Combust Inst* 2005, 30, 1155–1163.
24. Bounaceur, R.; Da Costa, I.; Fournet, R.; Billaud, F.; Battin-Leclerc, F. *Int J Chem Kinet* 2005, 37, 25–49.
25. Emdee, J. L.; Brezinsky, K.; Glassman, I. *Proc Combust Inst* 1990, 23, 77–84.
26. Emdee, J. L.; Brezinsky, K.; Glassman, I. *J Phys Chem* 1991, 95, 1626–1635.
27. Roubaud, A.; Minetti, R.; Sochet, L. R. *Combust Flame* 2000, 121, 535–541.
28. Roubaud, A.; Lemaire, O.; Minetti, R.; Sochet, L. R. *Combust Flame* 2000, 123, 561–571.
29. Gregory, D.; Jackson, R. A.; Bennet, P. J. *Combust Flame* 1999, 118, 459–468.
30. Gail, S.; Dagaut, P. *Combust Flame* 2005, 141, 281–297.
31. Gail, S.; Dagaut, P. In *Proceedings of the European Combustion Meeting*, Louvain-la-Neuve, Belgium, April 3–6, 2005.
32. Kee, R. J.; Rupley, F. M.; Miller, J. A. In *Sandia Laboratories Report*, S 89-8009B, 1993.
33. Fournet, R.; Baugé, J. C.; Battin-Leclerc, F. *Int J Chem Kinet* 1999, 31, 361–379.
34. Belmekki, N.; Glaude, P. A.; I. Da Costa, I.; Fournet, R.; Battin-Leclerc, F. *Int J Chem Kinet* 2002, 34, 172–183.
35. Barbé, P.; Battin-Leclerc, F.; Côme, G. M. *J Chim Phys* 1995, 92, 1666–1692.
36. Baulch, D. L.; Cobos, C. J.; Cox, R. A.; Franck, P.; Hayman, G. D.; Just, Th.; Kerr, J. A.; Murrells, T. P.; Pilling, M. J.; Troe, J.; Walker, R. W.; Warnatz, J. *Combust Flame* 1994, 98, 59–79.
37. Tsang, W.; Hampson, R. F. *J Phys Chem Ref Data* 1986, 15, 1087–1279.
38. Troe, J. *Ber Buns Phys Chem* 1974, 78, 478–485.
39. Muller, C.; Michel, V.; Scacchi, G.; Côme, G. M. *J Chim Phys* 1995, 92, 1154–1177.
40. Benson, S. W. In *Thermochemical Kinetics*, 2nd ed.; Wiley: New York, 1976.
41. Pollack, S. K.; Raine, B. C.; Hehre, W. J. *J Am Chem Soc* 1981, 103, 6308–6313.
42. Da Costa, I.; Eng, R.; Gebbert, A.; Hippler, H. *Proc Combust Inst* 2000, 28, 1537–1543.
43. Fernandes, R. X.; Gebert, A.; Hippler, H. *Proc Combust Inst* 2002, 29, 1337–1343.
44. Marinov, N. M.; Pitz, W. J.; Westbrook, W. K.; Castaldi, M. J.; Senkan, S. M. *Combust Sci Technol* 1996, 116–117, 211–287.
45. Roth, W. R.; Scholz, B. P. *Chem Ber* 1981, 114, 3741–3750.
46. Tsang, W.; Cui, J. P. *J Am Chem Soc* 1990, 112(5), 1665–1671.
47. Ingham, T.; Walker, R. W.; Woolford, R. E. *Proc Combust Inst* 1994, 25, 767–774.
48. Allara, D. L.; Shaw, R. *J Phys Chem Ref Data* 1980, 9, 523–559.
49. Hippler, H.; Seisel, S.; Troe, J. *Proc Combust Inst* 1994, 25, 875–882.
50. Errede, L. A.; DeMaria, F. *J Phys Chem* 1962, 66, 2664–2672.